EMI Spectral Aggregation of Modulation Schemes in a lab-based DC Microgrid

Angel Pena-Quintal
GGIEMR
University of Nottingham
Nottingham, The UK
angel.penaquintal1@nottingham.ac.uk

Arun Khilnani
GGIEMR
University of Nottingham
Nottingham, The UK
arun.khilnani@nottingham.ac.uk

Leonardo Sandrolini
DEI
University of Bologna
Bologna, Italy
leonardo.sandrolini@unibo.it

Mark Sumner
PEMC
University of Nottingham
Nottingham, The UK
mark.sumner@nottingham.ac.uk

David Thomas
GGIEMR
University of Nottingham
Nottingham, The UK
david.thomas@nottingham.ac.uk

Steve Greedy
GGIEMR
University of Nottingham
Nottingham, The UK
steve.greedy@nottingham.ac.uk

***Abstract*—DC Microgrid research has developed in the recent years following the increasing integration of power electronic based switching devices at the point of common coupling in DC grids. This has led to electromagnetic interference problems caused by the spectral aggregation of conducted emissions in the low-frequency range (2-150 kHz). To investigate this, a framework for understanding spectral aggregation resulting from the multiple switching harmonics from the interconnected DC grid devices is analysed. In this work, three modulation techniques are applied to identical & parallel connected DC/DC converters forming a lab-based DC grid. The harmonics are then analysed for spectral aggregation using an EMI receiver. This provides insights into the spectral aggregation of conducted emissions in the low-frequency range to promote electromagnetic compatibility and further facilitate a possible framework for standardisation of DC power quality.**

***Index Terms*—DC Microgrids, Spectral Analysis, Modulation, Spread Spectrum**

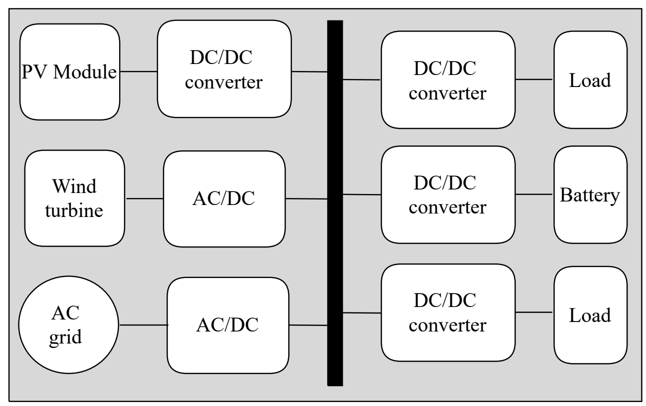

Fig. 1: Typical DC Microgrid set-up with the PCC [1]

I. Introduction

The increasing localised power generation has led to further integration of DC grid based Power Electronic Converters (PEC) into the main AC grid [1]. Due to the inherent switching frequencies of the converters, greater levels of Conducted Emissions (CE) are now reported at the Point of Common Coupling (PCC) in the low-frequency range, giving rise to Electromagnetic Interference (EMI) issues [2]. Further, the influence of CE and Radiated Emissions (RE) at low frequencies (up to 150 kHz) is reported to be detrimental on Power Line Communication (PLC) encouraging further investigations in the low-frequency range [3]. Given that the power converter switching frequencies are in the 2-150 kHz range, the spectral aggregation can compromise the signal integrity and communication reliability of the PLC based smart grids. The presence of converter switching frequencies and their harmonics in the 2-150 kHz range leads to spectral aggregation causing poor Electromagnetic Compatibility (EMC) between devices in the smart grids. In Europe, the frequency range for PLC is covered by standards such as the CENELEC A which has a frequency band from 3 to 95 kHz, CENELEC B ranging from 95 to 125 kHz, CENELEC C with a bandwidth from 125 kHz to 140 kHz and CENELEC D with a bandwidth from 140 to 148.5 kHz [4].

The spectral aggregation further can be inherently a result of modulation schemes of the converters. To promote EMC between converters in the DC grid through standards in the 2-150 kHz range, research about spectral aggregation is motivated. The aim of this paper is to analyse the spectral aggregation of three different applied modulation techniques in frequency-domain at a PCC in the CISPR-16 Band A frequency bandwidth for two identical & parallel connected DC/DC converters. This will help to understand how different modulation techniques can aggregate themselves over the same PCC which is something that can happen in modern smartgrids.

ETOPIA project research is funded by the European Union's Horizon 2020 research and innovation programme under the Marie Sklodowska-Curie grant agreement No 812753.

The rest of the paper is organised as follows. In Section II, the background of spectral aggregation is presented and theoretical aspects of the modulation schemes are explained with a focus on frequency domain effects by the common measurement techniques. Section III describes the experimental test set-up for the lab-based DC microgrid along with component description. The results for different modulation schemes are presented in Section IV. Finally, Section V presents the conclusions.

II. SPECTRAL AGGREGATION

The accumulation of different DC converter's harmonic indices and their multiples arising due to numerous switching frequencies from converters in a DC grid is termed as spectral aggregation of CE. In DC microgrids this aggregation results from a large number interconnected devices at the PCC with different switching frequencies and modulation techniques. A DC microgrid can have bi-directional power capability for the interconnected converters at the same PCC. A typical microgrid set-up with different interconnected devices at the same PCC (Fig.1) may have non-linear loads such as: Batteries, Chargers and Motors.

The accumulated distortion due to the spectral aggregation of an AC microgrid system with interconnected devices at the PCC is reported to decrease once a certain maximum number of devices are connected [3]. Any further addition of devices to the PCC interconnections leads to a decrease in the accumulative spectral aggregation possibly due to the capacitive nature of DC grids [5]. Moreover, DC microgrids are also expected to be capacitive in nature due to the presence of filtering from the interconnected power electronic converters. Hence, the behaviour of the DC grid from an EMC perspective tends to settle once a large number of converters have been connected.

To understand this effect in DC grids, a MATLAB/SIMULINK simulation based on buck converters was carried out by the authors considering the component values used for the experimental test set-up (which is explained in the next sections), the result is shown in Fig. 2. The simulation result shows the voltage measured at the PCC for the group of converters. We have considered the spectral aggregation of a DC grid with a similar approach that the one used in [5]. This approach is explained by the usage of ten interconnected converters at the same PCC with a random phase between them. In addition, all the converters are maintained at the same switching frequency (20 kHz) and have the same LC components. Furthermore, the DC link PCC is held with a large 4700 μF capacitance.

The increasing level of spectral aggregation can be noticed with the increasing number of connected converters, but tends to reach a maximum state possibly due to the increasingly capacitive nature of the DC grid. The spectral aggregation is observed to be a non-linear phenomenon due to the inherent non-linear nature of the power electronics converters leading to EMI issues within the DC microgrid. A functional DC/DC microgrid should consider EMI mitigation techniques such as filtering and active control to promote EMC and system stability.

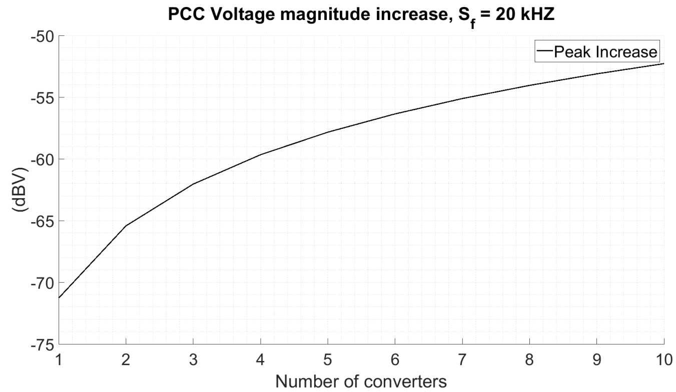

Fig. 2: Spectral aggregation of ten identical converters, S_f stands for switching frequency

A. Main PCC issues in microgrids

DC microgrids are robust systems that offer easiness of control (i.e no need for a base-frequency synchronisation) and can be applied with adequate filtering to enhance Power Quality (PQ). However, the lack of adequate filtering to attenuate frequencies present in the grid below or beyond a certain frequency range can be detrimental to system stability and PQ [6], [7]. This poor PQ in the DC grid results from the harmonics content (ripples) of the switching frequency termed as frequency beating. These beat frequencies when achieve the system's resonance frequency result in system instability. To measure these beat frequencies at the PCC in the Frequency Domain (FD), Fast Fourier Transform (FFT) can be effectively used. In fact, the most recent time-domain EMI receivers base their functioning on a rapid decomposition which is the Short-Time Fourier Transform (STFT) and windowing techniques over a certain time [8].

B. Limitation in Measurements

To accurately measure the spectral aggregation of CE of a converter as Device Under Test (DUT), a Line Impedance Stabilisation Network (LISN) can be used between the main power supply (either AC or DC) and the DUT. The LISN provides output impedance stability to the DUT to enable accurate and repeatable measurements in the prescribed frequency range. In Table I, commercial LISNs offering different frequency bandwidths are described.

The *MIL* is for *United States Military Standard* and establishes a basic topology for a LISN, with a 5μH and a 50μH inductors capable of providing stable impedance between 9-150 kHz and 150 kHz-30 MHz respectively [9]. The *Comité International Spécial des Perturbations Radioélectriques* (CISPR) too has a basic topology for a LISN, with a 50μH inductor capable of providing stable impedance between 9-150 kHz [10].Commercial LISNs applying these topologies are off-the-shelf products [11].

TABLE I: Bandwidth of Standard LISNs [12]

Sr. No	LISN Topology	Frequency Range
1	MIL-STD-461-G (50μH)	10 kHz to 10 MHz
2	MIL-STD-461-G (5μH)	150 kHz to 30 MHz
3	CISPR-22	150 kHz to 30 MHz
4	CISPR-16-1	9 kHz to 30 MHz

However, both the standards offer measurements from 9 kHz onward with a gap frequency between 2-9 kHz [10], [12]. Moreover, the drawbacks for using an AC topology specific LISN for DC grids are :

- The existing LISN topologies provide a stable input impedance to AC devices to ensure repeatable measurements for CE within the specified frequency range. The topology is specifically aimed at an inductive AC grid. DC grids are presumed to be largely capacitive as the outputs of converters are capacitive in nature [13].
- The commercial LISNs do not offer stable impedance to DC grids in the gap frequency range (2-9 kHz) with capacitive inputs.
- Depending on the configuration, the LISNs are either 1-θ or 3-θ devices along with a separate circuit for the neutral. The DC grid is a two-terminal topology with a positive and a negative DC link. For this reason a configuration that includes a LISN for the positive terminal and a LISN for the negative terminal should be used to accurately fix the impedance of the systems involved.

C. Spread-Spectrum Modulation scheme

Spread Spectrum has been used recently as an EMI mitigation technique that can assist to ensure the compliance of a device to a standardised limit for a given bandwidth. In general, it decreases a narrowband interfering signal to a spread spectrum signal. To achieve this, a frequency modulation of switching frequencies is carried out to control the EMI generated by the DC/DC converters. The effect of this procedure is the generation of a high and a low limit around the base frequency to be mitigated. This behaviour is better explained by Carson's rule which defines the bandwidth required of a communication channel for a carrier signal that is being modulated by many frequencies rather than a single one. The mathematical expression can be seen in Eq. 1.

$$f_{out} = f_b \pm \frac{\Delta f}{2} \cdot \epsilon(t), \quad (1)$$

wherein:

- f_b is the central or base frequency to be mitigated,
- f_{out} is the modulated switching frequency,
- Δf is the frequency deviation based on the spreading factor range defined (lower and higher limit) and,
- $\epsilon(t)$ is the driving signal to modulate the converter in frequency. This signal can be either periodic or non-periodic.

The driving signal is an important factor for addressing the shape of the results in the frequency domain and can be periodical or non-periodical [14].

The frequency deviation for the modulation schemes used for our research is considered only the 10% of the actual base frequency used for the deterministic case (20 kHz). This value was decided in order to maintain the system steady and to avoid chaotic behaviour in higher frequencies.

It has been widely discussed that the application of spreading techniques can decrease any level of interfering signal if a considerable spreading factor is used. However, this approach can generate issues on close and higher frequencies since spread spectrum redistributes the peak signal energy throughout the entire spectrum. The advantage of different spreading factors is not the take-to-home idea of this paper, in fact the main idea is to show the effect of aggregation when using only the 10% of the spreading factor.

D. Modulation schemes considered for the DC/DC converters

The three modulations chosen are given by Deterministic Modulation (DetM), Spread Spectrum Modulation (SSM), and Random Modulation (RM). The simplest SSM is based on a modulating sine wave of 20 Hz. This value of frequency has been chosen due to the stability of the readings obtained by the measuring equipment. Two things should be noted.

- The maximum switching frequency achieved is 21 kHz while the minimum switching frequency is 19 kHz for SSM and RM.
- The speed of the transition between these limits is given by the modulating sine for the SSM case, this means that there will be a complete cycle of the switching frequency every 2 kHz.

On the other hand, the RM used is based on an Uniform Distributed Random Signal. The generation of RM switching frequencies combinations can be seen in Fig. 3. The modulation schemes combinations are shown in Table II. For the tests, the voltage of the PCC is measured (V_{PCC}).

To gain understanding about different devices connected to a PCC in the CISPR-16 Band A, combinations of the three different modulation techniques mentioned before have been chosen. The results of these three modulations are shown initially for standalone converters. Then, combinations of modulation techniques are carried out.

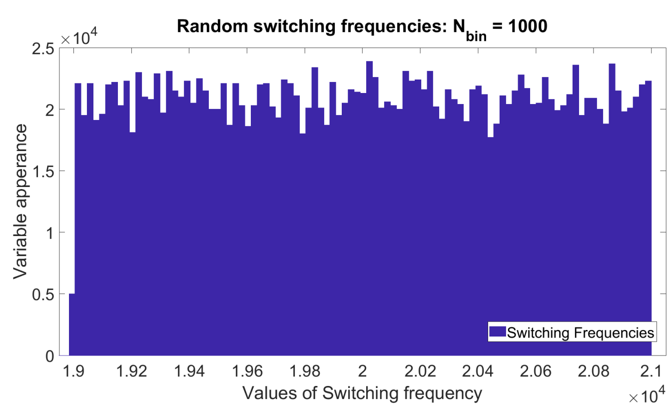

Fig. 3: Random switching frequencies generated by the PWM

TABLE II: Modulation schemes combination for the test

Modulation	V_{PCC}
DetM/DetM	✓
DetM/SSM	✓
DetM/RM	✓
RM/SSM	✓
RM/RM	✓

In Table II, the combination of SSM/SSM is not used because it can present a very specific case that will have very low probability of happening in a real test compared to deterministic and random combinations.

III. Experimental test set-up

The experimental test set-up is based on the usage of a LISN and an EMI receiver, both compliant with CISPR-16. The LISN provides isolation to the DC/DC converters which are considered as the DUT. The LISN filters the CE from the DC Power Supply to the converters, providing them a cleaner voltage and current in the frequency bandwidth 9 kHz to 150 kHz. The terminals connected from the power supply to the LISN are the 2 LISN circuits, this means one for the positive point of the power supply and the other to the negative point. The output voltage of the power supply has been set at 48 V.

The dwell time of the EMI receiver is configured at 200 ms to analyse the frequency band A of CISPR-16, this value has been chosen to have as an starting point similar to AC standards of PQ [15]. The Resolution Bandwidth frequency is 200 Hz according to CISPR 16 Band A (9 - 150 kHz). The spectral analysis relies on the results obtained from the EMI receiver. The block diagram of the experimental test set-up is shown in Fig. 4.

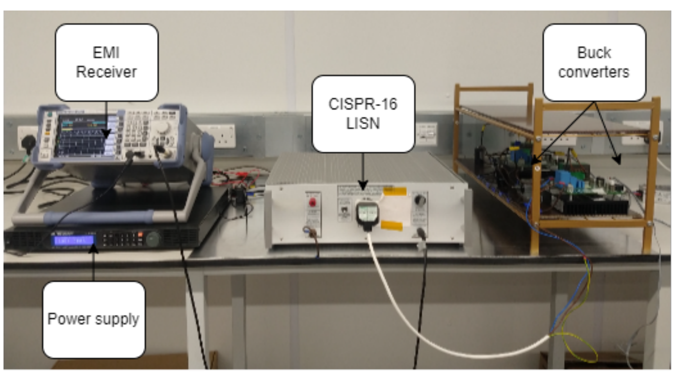

Fig. 4: Experimental test set-up

The DC/DC converter used is the asynchronous buck converter. The components such as capacitor, inductor, and resistor were chosen as similar as possible for the pair of converters. The main values are listed in Table III. The DC/DC converter offers flexibility to access for the controlling of the transistors. The transistor of the converter is being driven by a Texas Instruments board LAUNCHXL-F28379D. To achieve the correct controlling of the converters, Eq. 1 has been implemented in the Texas Instruments board.

TABLE III: DC converter main parameters

Component	**Value**
Input capacitor	5.1 μF
Output capacitor	470 μF
Inductor	1 mH
Resistor	10 Ω

IV. Results

The measured indices from the EMI receiver are Peak (PK), Quasi-Peak (QP), and Average (AV) detectors. The use of these three indices can help to determine the changes due to a different rate of change when frequency modulation techniques are used (SSM and RM). The EMI receiver was configured using a logarithmic sweep of 1%, this means that the frequency is incremented in 1% of the current frequency step. To compare 2 different cases the results will present the graphs for a single converter and two converters.

A. Frequency-domain results: Single converter

The results for the three different modulations schemes can be seen in Fig. 5. In these results the most important indices are given by a) Peak, b) Quasi-Peak, and c) Average detectors. The frequency band is between 18 kHz to 22 kHz to analyse the main switching frequency of the converter (20 kHz).

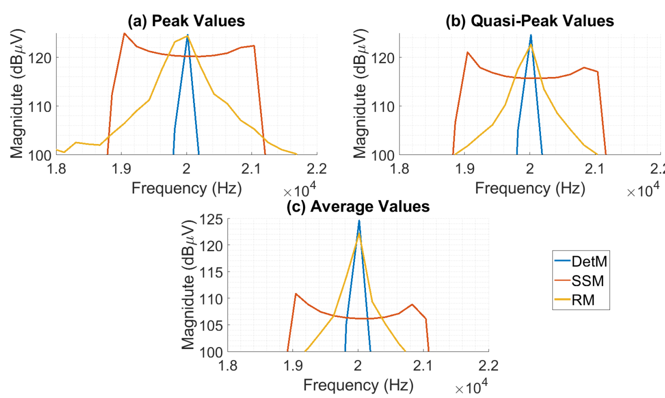

Fig. 5: Single converter: frequency-domain graphs obtained with the EMI receiver [18 kHz - 22 kHz]

In Fig. 5, there are important points to consider as follows.

- When SSM is used the value of the switching frequency presents a considerable decrease at the central modulated frequency (20 kHz), however there exists sidelobes with similar or even higher values when compared to the maximum frequency to mitigate. This is one drawback of the SSM with a sine wave as a modulating signal.
- The measured indices, follow the according rule given by CISPR-16 standard. This is, non-modulated behaviour (DetM) as $Peak = Quasi - Peak = Average$. On the other hand frequency-modulated behaviour (SS and RM) as $Peak > Quasi - Peak > Average$.

The spectrum between 9 kHz to 150 kHz for one converter is shown in Fig. 6. The results for the presented cases use the same main indices. In this figure, it can be noticed the frequency occupancy increase for higher switching frequencies such as 40 kHz, 60 kHz, 80 kHz, 100 kHz, 120 kHz 140 kHz.

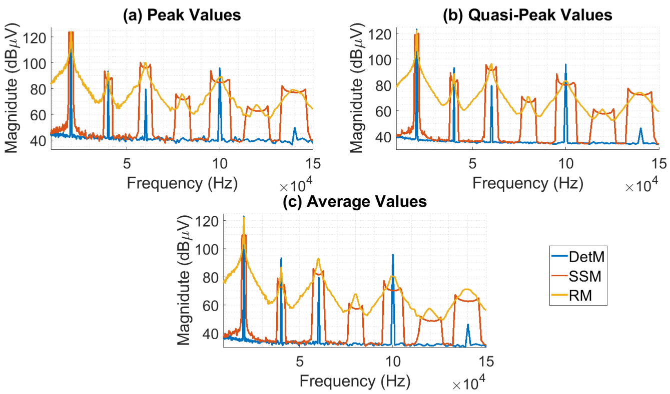

Fig. 6: Frequency-domain graphs obtained with the EMI receiver [9 kHz - 150 kHz]

In Table IV, the three different modulation techniques with the three main indices are shown. As can be seen, the results are similar between them. This is mainly caused by the use of only the 10% of the original base frequency. In reality, the use of this percentage is low if the objective is to obtain a peak decrease. On the other hand, a frequency deviation like the one used in the experimental test can be taken as a value in between deterministic modulation and spread spectrum.

TABLE IV: 1 converter: Modulation schemes results

1 converter	**Peak** ($dB\mu V$)	**QP** ($dB\mu V$)	**AV** ($dB\mu V$)
DetM	124.61	124.58	124.61
SSM	120.12	115.63	106.12
RM	124.35	122.59	122.17

B. Frequency-domain results: Two converters

The spectral aggregation of two converters with different combinations of modulations can be seen in Fig. 7, considering the three most important indices. The frequency band is between 18 kHz to 22 kHz.

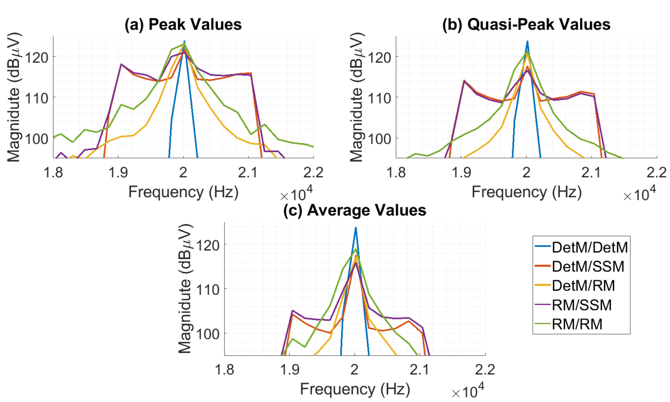

Fig. 7: Frequency-domain graphs obtained with the EMI receiver [18 kHz - 22 kHz]

While in Fig. 8 can be seen the obtained spectrum between 9 kHz - 150 kHz for the five combinations analysed.

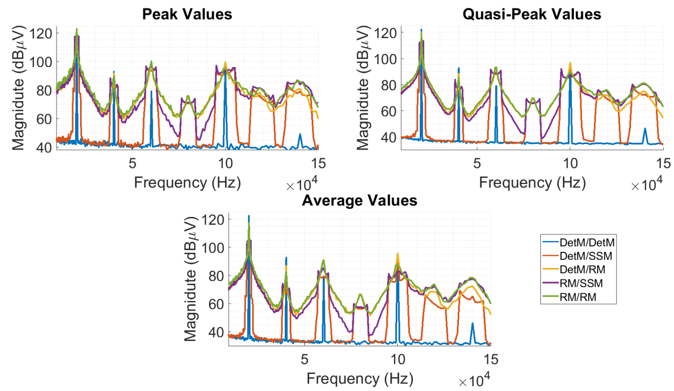

Fig. 8: Frequency-domain graphs obtained with the EMI receiver [9 kHz - 150 kHz]

The use of different combinations can provide interesting results of how different modulations schemes generate different shapes when analysing the spectral content measured by the EMI receiver. As was expected, the usage of Random Modulation increases the magnitude in the frequency range surrounding the peak of the base switching frequency. However, when it is combined with a sine modulated scheme the shape remains similar within the limits of the spreading factor.

On the other hand, the effect of EMI mitigation is very low if we compare the different modulations used. Nevertheless, this is an important point in order to compare the different modulations and define which case shows advantages over others since they have the exact same frequency deviation.

The spreading techniques are mainly based on the assumption that the bigger the factor to spread the lower the peak value is, but this relationship is non linear. Similar results of peak decrease and sidelobes generation can be discussed for the different combinations of modulation schemes applied to the pair of converters. The mitigation tends to show small but consistent values. Similarly, the occupancy of the bandwidth tends to increase for higher switching frequencies.

This is a drawback of using frequency modulation techniques for DC/DC converters, the application of these mitigation techniques must be applied only when required and under extensive knowledge of the entire system.

In Table V, Table VI, Table VII and, Table VIII can be seen the indices values when compared to the baseline case of using two converters with DetM.

TABLE V: Combination: DetM/SSM

2 converters	**PK** ($dB\mu V$)	**QP** ($dB\mu V$)	**AV** ($dB\mu V$)
DetM/DetM	123.81	123.78	123.81
DetM/SSM	121.65	117.60	117.50
Diff	2.15	6.18	6.31

The SSM and RM schemes are considered close to the frequency of 20 kHz. One can notice that the results obtained in Table IV, Table IV and Table V which show a small difference when compared, one of the main causes it could be given by the usage of input capacitors in the converters.

TABLE VI: Combination: DetM/RM

2 converters	**PK** ($dB\mu V$)	**QP** ($dB\mu V$)	**AV** ($dB\mu V$)
DetM/DetM	123.81	123.78	123.81
DetM/RM	123.30	120.76	117.18
Diff	0.51	3.02	6.63

TABLE VII: Combination: RM/SSM

2 converters	**PK** ($dB\mu V$)	**QP** ($dB\mu V$)	**AV** ($dB\mu V$)
DetM/DetM	123.81	123.78	123.81
RM/SSM	121.01	116.61	115.81
Diff	2.8	7.17	8.0

TABLE VIII: Combination: RM/RM

2 converters	**PK** ($dB\mu V$)	**QP** ($dB\mu V$)	**AV** ($dB\mu V$)
DetM/DetM	123.81	123.78	123.81
RM/RM	123.10	121.34	118.93
Diff	0.71	2.47	4.88

V. Conclusion and future work

The use of different modulation techniques showed that using the 10% of the base signal to aggregate the spectral content of 1 and 2 converters does not change the indices values in a considerable way for the main switching frequency. On the other hand, the use of different combinations will have an affect on the shape calculated by the EMI receiver. In fact, all the cases when random modulation was used the energy of the narrowband signal increases considerably. This can be a problem to nearby frequencies.

The effect of generating issues can be noticed in higher frequency bands. The mitigation technique should not only have to consider the main switching frequency to be mitigated, but also the impact of this technique for a different bandwidth. An important point to mention is the lack of measurements below 9 kHz which in fact can not be obtained by using the experimental test set-up carried out.

The future work will be focused on the understanding of different converters with different switching frequencies and how one random modulated converter can be used as a sum of plenty of different converters with deterministic modulation. In addition an analysis based on Power Quality should be needed to determine the main advantages and disadvantages for the different modulations used. A complete sweep analysis for the spreading coefficient will give a better understanding of the spectral aggregation effect in frequency modulated DC/DC converters.

References

[1] D. Kumar, F. Zare, and A. Ghosh, “Dc microgrid technology: System architectures, ac grid interfaces, grounding schemes, power quality, communication networks, applications, and standardizations aspects,” *IEEE Access*, vol. 5, pp. 12 230–12 256, 2017.

[2] D. Thomas, “Conducted emissions in distribution systems (1 khz–1 mhz),” *IEEE Electromagnetic Compatibility Magazine*, vol. 2, no. 2, pp. 101–104, 2013.

[3] S. K. Rönnberg, M. H. Bollen, H. Amaris, G. W. Chang, I. Y. Gu, Łukasz H. Kocewiak, J. Meyer, M. Olofsson, P. F. Ribeiro, and J. Desmet, “On waveform distortion in the frequency range of 2khz–150khz—review and research challenges,” *Electric Power Systems Research*, vol. 150, pp. 1–10, 2017. [Online]. Available: https://www.sciencedirect.com/science/article/pii/S0378779617301864

[4] C. Cano, A. Pittolo, D. Malonem, L. Lampe, A. M. Tonello, and A. G. Dabak, “State of the art in power line communications: From the applications to the medium,” *Journal on Selected Areas in Communications*, vol. 34, pp. 1935–1952, 2016. [Online]. Available: https://www.sciencedirect.com/science/article/pii/S0378779620301310

[5] Ángela Espín-Delgado, S. Rönnberg, T. Busatto, V. Ravindran, and M. Bollen, “Summation law for supraharmonic currents (2–150 khz) in low-voltage installations,” *Electric Power Systems Research*, vol. 184, p. 106325, 2020. [Online]. Available: https://www.sciencedirect.com/science/article/pii/S0378779620301310

[6] X. Yue, F. Zhuo, S. Yang, Y. Pei, and H. Yi, “A matrix-based multifrequency output impedance model for beat frequency oscillation analysis in distributed power systems,” *IEEE Journal of Emerging and Selected Topics in Power Electronics*, vol. 4, no. 1, pp. 80–92, 2016.

[7] X. Yue, D. Boroyevich, F. C. Lee, F. Chen, R. Burgos, and F. Zhuo, “Beat frequency oscillation analysis for power electronic converters in dc nanogrid based on crossed frequency output impedance matrix model,” *IEEE Transactions on Power Electronics*, vol. 33, no. 4, pp. 3052–3064, 2018.

[8] T. D. S. Braun and P. Russer, “A real-time time-domain emi measurement system for full-compliance measurements according to cispr 16-1-1,” *IEEE Transactions on Electromagnetic Compatibility*, vol. 50, 2, pp. 259–267, 2008.

[9] MIL-STD-461G, “Department of defence interface standard: Requirements for the control of electromagnetic interference characteristics of subsystems and equipment,” United States Military Standard, Tech. Rep., 2015.

[10] CISPR16-1-2, “Specification for radio disturbance and immunity measuring apparatus and methods – part 1-2: Radio disturbance and immunity measuring apparatus - coupling devices for conducted disturbance measurements,” International Electrotechnical Commission, Tech. Rep., 2014+AMD1:2017.

[11] S. GmbH, “Schwarzbeck lisn.” [Online]. Available: http://schwarzbeck.de/en/lisn-line-impedance-stabilisation-networks/v-lisn-en/v-lisn-cispr-16-1-2/307-nslk-8127.html

[12] A. Khilnani, L. Wan, M. Sumner, D. Thomas, A. Hamid, and F. Grassi, “Conducted emissions measurements in dc grids: Issues in applying existing lisn topologies and possible solutions,” in *2021 IEEE 15th International Conference on Compatibility, Power Electronics and Power Engineering (CPE-POWERENG)*, 2021, pp. 1–6.

[13] M. Liserre, F. Blaabjerg, and A. Dell’Aquila, “Step-by-step design procedure for a grid-connected three-phase pwm voltage source converter,” *International Journal of Electronics*, vol. 91, pp. 445 – 460, 2004.

[14] R. R. F. Pareschi and G. Setti, “Emi reduction via spread spectrum in dc/dc converters: State of the art, optimization, and tradeoffs,” *IEEE Access*, vol. 3, pp. 2857–2874, 2015.

[15] I.-I. E. Commission, “Testing and measurement techniques – general guide on harmonics and interharmonics measurements and instrumentation, for power supply systems and equipment connected thereto,” International Electrotechnical Commission, Tech. Rep., 2002.